JMEPEG (2017) 26:478–487
DOI: 10.1007/s11665-016-2461-1

1059-9495/$19.00

Effect of Spheroidizing Annealing on Microstructure and Mechanical Properties of High-Carbon Martensitic Stainless Steel 8Cr13MoV

Wen-Tao Yu, Jing Li, Cheng-Bin Shi, and Qin-Tian Zhu

(Submitted May 16, 2016; in revised form November 19, 2016; published online December 21, 2016)

The effects of holding time during both austenitizing and spheroidizing on microstructure and mechanical properties of high-carbon martensitic stainless steel 8Cr13MoV were experimentally studied. The results showed that the amount of carbides and the proportion of fine carbides decrease first and then increase with the increase in austenitizing time (t_1) in the case of short spheroidizing time (t_2), whereas the amount of the lamellar carbides increases. In the case of long t_2, both the amount of carbides and the proportion of fine carbides decrease, and the amount of the lamellar carbides did not increase. The hardness of the steel decreases first and then increases with the increase of t_1. Under the conditions of different t_1, the change in the size of carbides and hardness of the steel show a same trend with the variation of t_2. The size of spheroidized carbides increases, whereas the hardness of the steel decreases with increasing t_2. The longer the holding time of austenitizing, the higher is the spheroidizing rate at the earlier stage. However, the spheroidizing rate shows an opposite trend with t_1 at the later stage of spheroidizing. The effect of cooling rate on microstructure is similar with t_2. With increasing cooling rate, the dimension of carbides became smaller, and the amount of lamellar carbides increased. The elongation of the sample fracture exhibits no corresponding relationship with holding time, whereas it is closely related to the precipitation of secondary carbides caused by the alloying elements segregation.

Keywords carbides, high-carbon martensitic stainless steel, mechanical properties, microstructure, spheroidizing annealing

1. Introduction

In view of their superior hardness, strength and abrasive resistance, martensitic stainless steels have been widely used as steam turbine components, high pressure vessel and knives materials (Ref 1-3). As a high-carbon martensitic stainless steel, 8Cr13MoV is raw material of high-grade knives and scissors. Because martensite transformation could be achieved under air-cooling condition, spheroidizing annealing should be performed for 8Cr13MoV steel prior to cold rolling. The purpose of spheroidizing annealing is to induce the precipitation of carbon as spherical carbides and distribute evenly in ferritic matrix, which could lower the hardness, improve the plasticity, as well as prevent edge crack and fracture of the steel during cold rolling process (Ref 4, 5). In the case of the same volume fraction of carbides, the larger of the carbides size is, the lower of the steel hardness is (Ref 6).

There are three spheroidizing annealing practices, namely (I) holding at the temperature below Ac_1, (II) repeated heating around Ac_1, (III) heating above Ac_1 and then cooling to the temperature below Ac_1, followed by holding at this temperature (Ref 7). Finally, the steel was cooled at a very small cooling rate in these three processes, inducing the formation of fine carbides. The growth and spheroidization of these carbides could be achieved by eutectoid transformation under a specified condition. It is named divorced eutectoid transformation (Ref 8, 9), which is similar with the eutectoid transformation occurred during liquid steel solidification. Although many studies on spheroidizing annealing have been reported, spheroidizing annealing for specified steel is largely different due to the variation of alloy elements contents in different steels (Ref 10, 11). The aforementioned second and third spheroidizing annealing practice with a small adjustment is usually applied to martensitic steel.

Only a few studies have been reported in studies to expound the technique of heat treatment of high-carbon martensitic stainless steels used as high-grade knives and scissors raw materials. Most of these previous studies are focused on the quench and tempering of high-carbon martensitic stainless steels. Spheroidizing annealing after hot rolling has an important effect on the processability and rolling yield. The present study was conducted to reveal the effects of holding time during both austenitizing and spheroidizing and cooling rate on the microstructure and mechanical properties of high-carbon martensitic stainless steel 8Cr13MoV.

2. Experimental

2.1 Raw Materials

The raw materials of 8Cr13MoV steel produced by ESR were forged into the slab of 200 mm × 150 mm × 30 mm. The as-cast ESR ingots were forged after being held at 1200 °C for 120 min. The forging finish temperature was no lower than

Wen-Tao Yu, Jing Li, Cheng-Bin Shi, and **Qin-Tian Zhu**, State Key Laboratory of Advanced Metallurgy, University of Science and Technology Beijing (USTB), Beijing 100083, China. Contact e-mail: ywt82@163.com.

Table 1 Chemical composition of 8Cr13MoV steel (mass%)

C	Cr	Mo	Mn	Si	V	Ni	P	S	Fe
0.775	14.68	0.213	0.458	0.333	0.182	0.157	0.031	0.004	Bal.

Table 2 Experimental conditions in each experiment

	Group, t_1/min		
Group, t_2/min	D (45)	E (90)	F (135)
A (45)	1#	4#	7#
B (90)	2#	5#	8#
C (135)	3#	6#	9#

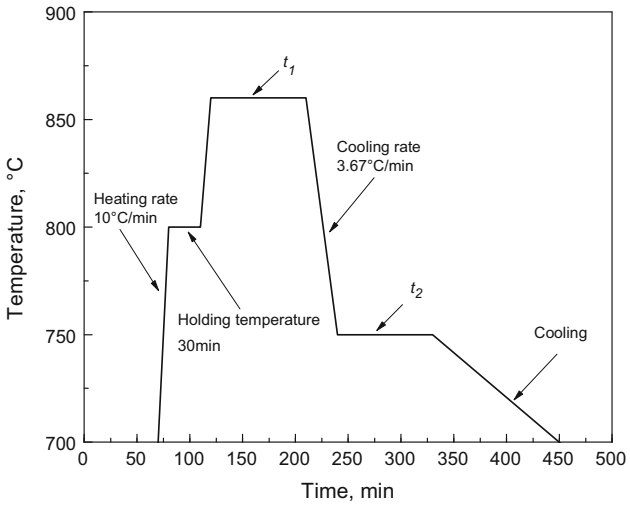

Fig. 1 Schematic diagram of thermomechanical test profile of spheroidizing annealing

Table 3 Experimental parameters

Sample	Sampling, time/min	Heat treatment process		Final temperature before sampling, °C
		Temperature, °C	Holding, time/min	
10#	165	860	45	860
11#	210	860	90	860
12#	255	860	135	860
13#	285	750	0	750
14#	375	750	90	750
15#	495	Cooling time: 120 min		701

800 °C. The metal samples of 100 mm × 45 mm × 30 mm that were cut from the slab were prepared for annealing experiments. The chemical composition of the 8Cr13MoV steel is given in Table 1. Ac_1 of the studied steel is about 840 °C.

2.2 Experimental Procedure

The annealing experiments were conducted using an electrical resistance furnace. The holding time of annealing was set at 1.5 to 2.5 min/mm according to the thickness of steel sample. Three holding times were applied for each test temperature. The austenitizing time and spheroidizing time were designated as t_1 and t_2, respectively. To investigate the effect of t_1 and the t_2 on microstructure and mechanical properties of steel, the experiments were classified as six groups. The experimental scheme is listed in Table 2. The test profile for spheroidizing annealing is schematically illustrated in Fig. 1. In the present work, 860 °C and 750 °C were selected as the holding temperatures of austenitizing and spheroidizing, respectively. After the holding of spheroidizing, the sample was cooled at a cooling rate of 25 °C/h in each experiment.

The influence of holding time on microstructure was analyzed according to the experimental scheme shown in Table 3. Austenitizing time and spheroidizing time were 135 and 90 min, respectively. Firstly, the samples were heated in the heating furnace. The samples were taken out after different holding time and quenched in cooling water after various heat treatments for keeping the original microstructure and morphology. Subsequently, the distribution of carbides in the steel was analyzed.

In order to verify the influence of different holding times of spheroidizing on microstructure and morphology of carbides, two groups of samples with t_1 = 135 min and t_2 = 45 min were studied. The cooling rate was 25, 50, 100 and 250 °C/h, respectively. The samples were designated as 16#, 17#, 18# and 19#, respectively.

2.3 Microscopic Observation of the Annealed Steel and Tensile Fracture

The microstructure of martensitic stainless steel before annealed consists of martensite, retained austenite, primary carbides as well as a few secondary carbides, as shown in Fig. 2. After spheroidizing annealing, the Rockwell hardness of the steel sample was measured. Three measurements were conducted for each sample to obtain an average value of hardness. The annealed samples were etched with a solution of alcohol, hydrochloric acid and ferric chloride at room temperature for analyzing the microstructure using scanning electron microscope (SEM). The carbides in the annealed steel samples were characterized by image analysis software.

The ESR ingot and spheroidizing annealed steel plates were sampled and machined to Ø8 mm × 80 mm tensile samples based on the Chinese national standard GBT228-2002. The mechanical properties were tested by universal material testing machine. The tensile fractures were observed using SEM.

2.4 The Determination of Carbide Type

Two samples of the spheroidizing annealing process were selected. Firstly, the carbide precipitate was extracted by means of carbon replica method. And then, transmission electron microscopy (TEM) electron diffraction method was employed to determine the transformation of carbide type before and after the spheroidization.

3. Results

3.1 Effect of Austenitizing Time on the Microstructure of Annealed Steel

As shown in Fig. 3, the microstructure of all these annealed samples consists of primary carbides, granular, lamellar, short rod-like carbides and ferritic matrix. The primary carbides are formed during solidification of liquid steel. These carbides remain in the steel after forging and annealing, as indicated by arrows in Fig. 3(a). A small amount of carbides show short rod-like or chain-like, indicating incomplete spheroidization of these carbides. In addition, a few carbides are lamellar in morphology, as labeled by arrows in Fig. 3(c).

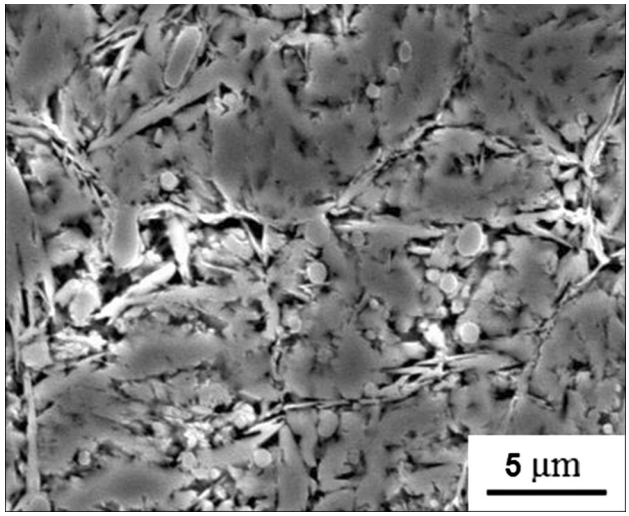

Fig. 2 Microstructure of the steel after forging

The microstructure characteristics of the sample, at the holding time of austenitizing t_1 45 min, among various group are identical. The size of carbides is uneven. Many fine carbides were observed. The carbides smaller than 0.2 μm are regarded as the fine ones. Figure 4(a) shows the proportion of fine carbides to the total amount of carbides. Taking the total amount of carbides in sample 1# as a base, the ratio of the amount of carbides in other samples to that in sample 1# is shown in Fig. 4(b). At t_1 of 90 min, the proportion of fine carbides in the samples of group A decreased from 46.94 to 38.31%, and the amount of carbides decreased to 19.31%. The amount of carbides in sample 7# increased slightly with time. The amount of lamellar carbides in sample 7# is greater than that in samples 1# and 4#. The amount of carbides in sample 8# increased by 7.41% compared with that in sample 5#. The amount of carbides in sample 9# is least in this group, whereas the size of the carbides is largest.

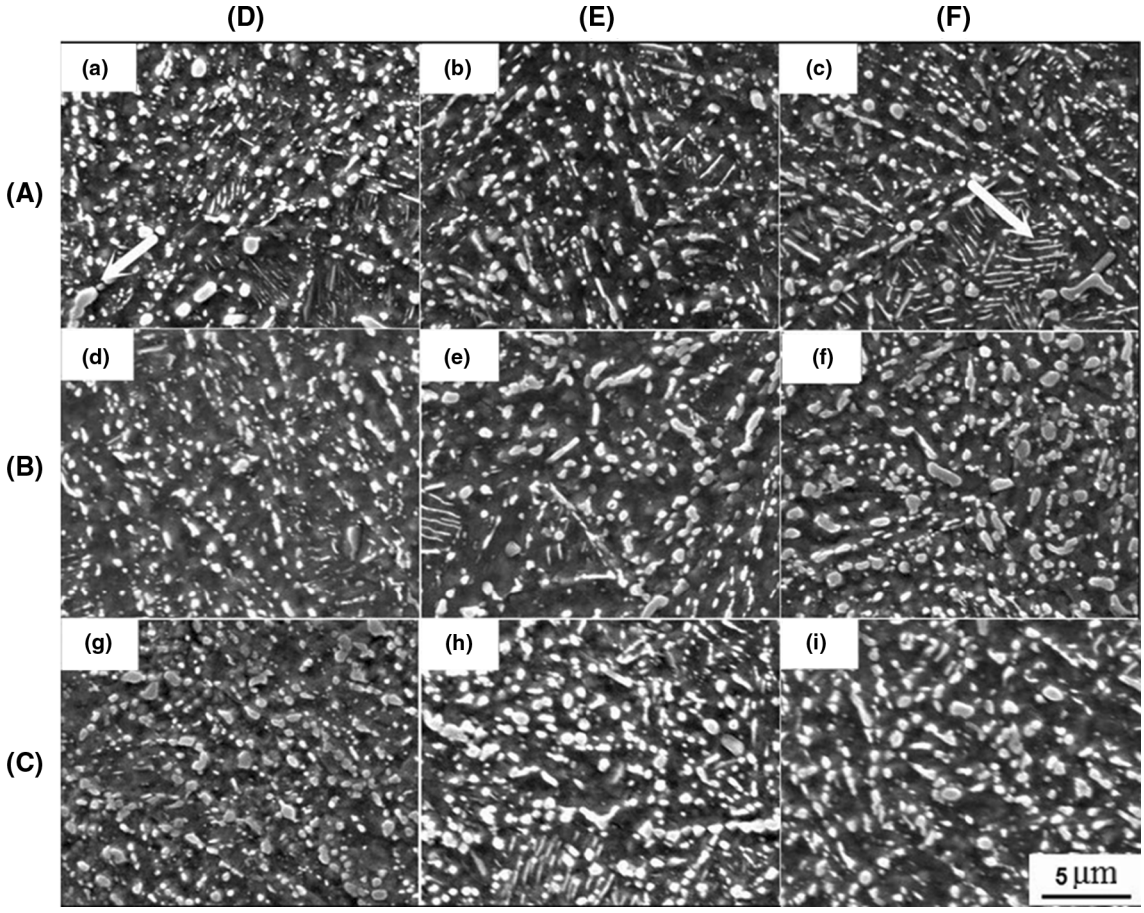

Fig. 3 SEM images of specimens holding for different t_1 and t_2: (a) 45 and 45 min, (b) 90 and 45 min, (c) 135 and 45 min, (d) 45 and 90 min, (e) 90 and 90 min, (f) 135 and 90 min, (g) 45 and 135 min, (h) 90 and 135 min, (j) 135 and 135 min, as shown in Fig. 3, the capital letters before each line and row are their group numbers

3.2 Effect of Spheroidizing Time on the Microstructure of Annealed Steel

It can be seen from Fig. 3, the size of carbides in these samples increases with the increase of t_2. Taking the samples in group F as an example, the average size of carbides is 0.47, 0.54 and 0.57 μm, respectively. The spheroidized degree of carbides is higher with time progresses, whereas the amount of carbides decreases. The volume fraction of carbides is nearly constant (about 30%).

3.3 Transformation of Carbide Type During Spheroidizing Annealing Process

The equilibrium phase formation and their fraction in 8Cr13MoV steel during liquid steel solidification and cooling were calculated using Thermo-Calc software, as shown in Fig. 5. Under the condition of equilibrium solidification, M_7C_3 formed from austenite and then transformed to $M_{23}C_6$. According to previous studies (Ref 12, 13), M_7C_3 type is the main carbides in 8Cr13MoV, besides a few $M_{23}C_6$ type. As shown in Fig. 5, in the temperature range of forging, these two types of carbides may transform to each other. In addition, dislocation and subboundary formed due to the existence of exogenous force and temperature change during forging. New type of carbides may form at these positions. The carbides are mainly $M_{23}C_6$ type in the temperature range of spheroidizing annealing, indicating the transformation of other types of carbides to $M_{23}C_6$.

After forging, primary carbides were crushed, but still large. These carbides would not be transformed during annealing process (Ref 14). Besides, lamellar carbides precipitated along the grain boundary and granular carbides also existed in the primary samples. TEM images and carbide diffraction pattern are shown in Fig. 6(a) and (b). Lamellar carbides with the perpendicular [0 1 2] were cementite M_3C. Granular carbides with the perpendicular [0 2 3] were $M_{23}C_6$. After spheroidizing annealing, the type of carbide in sample 15# was analyzed. The type of long strip and granular carbides were $M_{23}C_6$ as shown in Fig. 6(c) and (d). It was considered that carbides transformed completely from M_3C to $M_{23}C_6$.

3.4 Effect of Spheroidizing Time on the Mechanical Property of Annealed Steel

In the practical production, low hardness and good plasticity of steel after hot rolling followed by spheroidizing annealing are expected in order to obtain excellent processability of the steel during cold rolling. Therefore, hardness measurement and tensile test of the steel after spheroidizing annealing were carried out. The hardness of all annealed steel samples is listed in Table 4.

The hardness variation of annealed samples with the holding time of spheroidizing t_1 is shown in Fig. 7. The hardness of annealed samples decreases first and then increases with t_1. The value of hardness is lowest at t_1 of 90 min. The tensile strength of each sample at different holding time is also shown in Fig. 7. The tensile strength of each sample exhibits identical trend as its hardness does. This finding is consistent with the results reported by others (Ref 15).

The plasticity of steel generally increases with the decrease in hardness (Ref 16). But the current results show that the relationship between the hardness of the steel and the elongation after fracture is unapparent, as shown in Fig. 8. It may result from the presence of nonmetallic inclusions and brittle precipitates with large size, especially primary carbides in the steel. It is widely accepted that primary carbides have higher hardness than steel matrix (Ref 17). Therefore, these primary carbides could act as breakage initiation sites during rolling and specific machining of this high-carbon steel.

3.5 Effect of Spheroidizing Time on the Mechanical Property of Annealed Steel

Figure 9 presents the hardness and tensile strength of each annealed sample at different holding time t_2. As can be seen, both the hardness and tensile strength of each sample decreased as the time passed. Combined with the microstructure observations

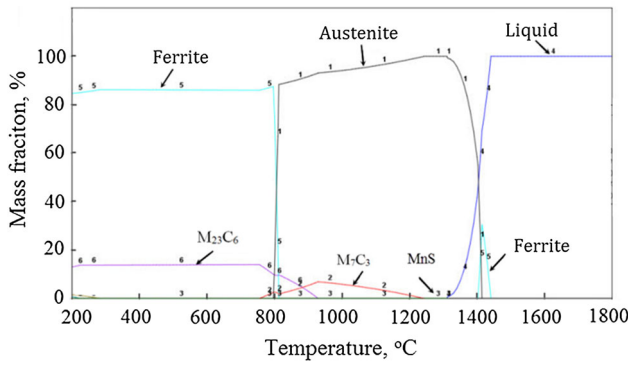

Fig. 5 Equilibrium phase precipitation in 8Cr13MoV steel calculated using Thermo-Calc

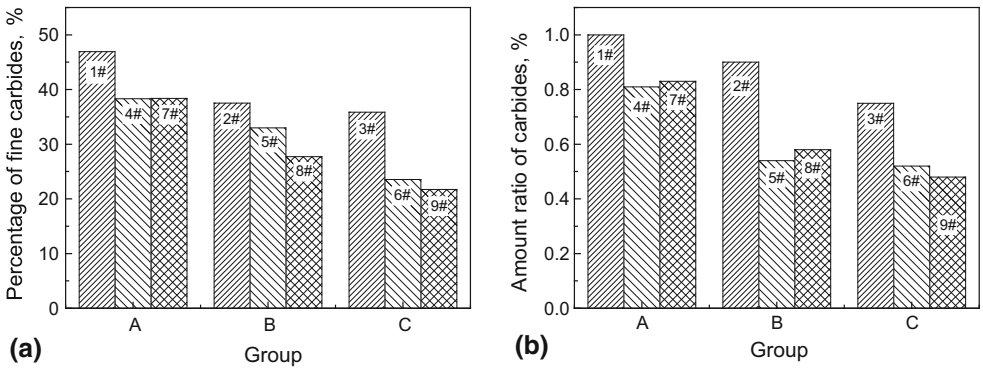

Fig. 4 (a) Proportion of fine carbides to the total amount of carbides, (b) The comparison of carbides amount in different samples (the amount of carbides in sample 1# was taken as a base for comparison)

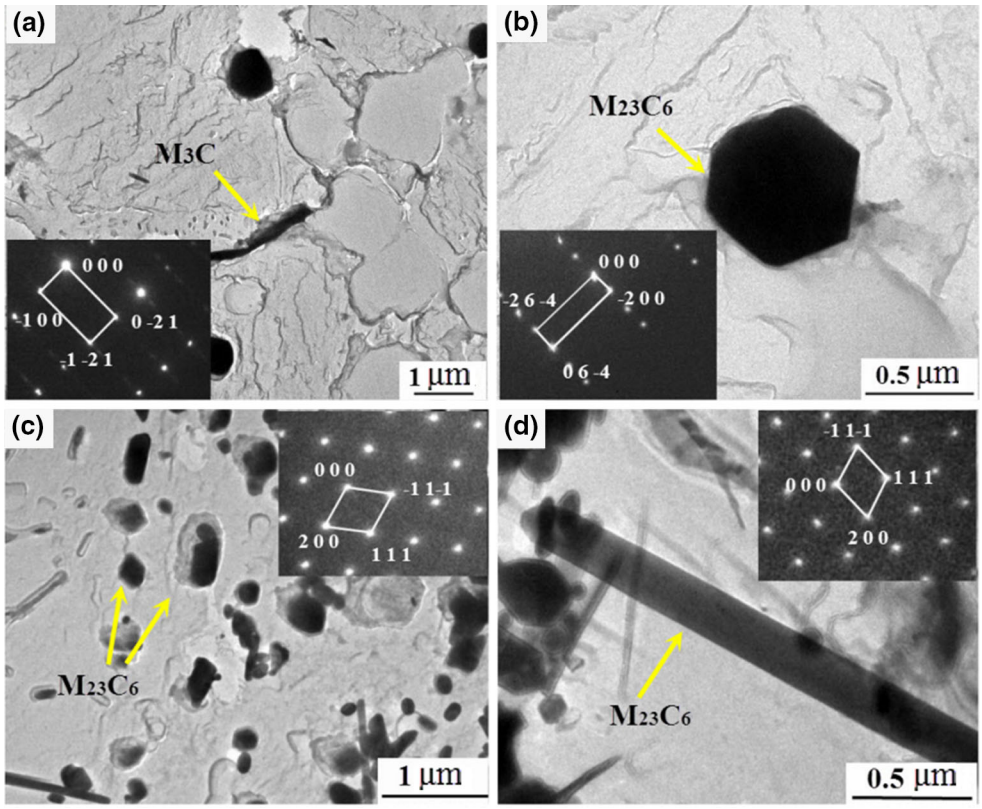

Fig. 6 TEM micrograph showing the microstructure and diffraction patterns of carbides: (a) lamellar boundary carbides of sample before spheroidizing, (b) granular carbides of sample before spheroidizing, (c) granular carbides of sample 15#, (d) long strip carbides in sample 15#

Table 4 Hardness of annealed steel samples (HRB)

	Group, t_1/min		
Group, t_2/min	D (45)	E (90)	F (135)
A (45)	95.56 (1#)	91.43 (4#)	93.71 (7#)
B (90)	95.22 (2#)	89.65 (5#)	89.95 (8#)
C (135)	92.65 (3#)	88.05 (6#)	89.71 (9#)

shown in Fig. 9, it can be deduced that the hardness of each annealed sample decreases with the increase in spheroidized degree of carbides. If the growth rate of carbides was used to reflect these changes in steel hardness, the growth rate of carbides in the steel samples of group E and F decreases with time goes, whereas the growth rate of carbides in the steel samples of group D increases. From 45 to 90 min of t_2, the growth rate of carbides in the steel samples follows the order: group E > group F > group D. The growth rate of carbides in the steel is in the order of group D > group F > group E when the holding time t_2 progresses from 90 to 135 min. This is closely related to the difference in t_1 among three groups. Further discussion will be given later.

4. Discussions

4.1 The Differences of the Microstructure Change with t_1 in Different Group

Although the hardness of all samples in group A-C decreased first and then increased, the microstructure of the samples among these groups was not the same, especially the last sample in each group. The microstructure in sample 7# contained more lamellar carbides, and the microstructure in sample 8# contained some small carbides. The microstructure of sample 9# had no obvious change compared with 6# sample. Samples 7#, 8# and 9# all belonged to F group, and the great microstructure difference was directly linked to t_2 obviously.

In order to analyze the effect of holding time of austenitizing and spheroidizing on microstructure, the samples in different annealing time were directly quenched in water and then analyzed to observe the morphology of carbides. The SEM images of samples are shown in Fig. 10. With the increase in t_1, the dissolution of carbides occurs, of which the small carbides were dissolved preferentially. Consequently, the spaces where exhibited large spacing among carbides formed (named large spacing thereinafter) due to the dissolution of carbides, which was visible in Fig. 10(c). Lamellar carbides were generated easier in these spaces (Ref 18). When the sampling temperature cooled from 860 to 750 °C, the matrix transformed from austenite to pearlite (ferrite + carbide). Meanwhile, primary carbides would grow up and new carbides would precipitate. As shown in Fig. 10(d), in the samples was cooled from 860 to 750 °C, the amount of carbides increased greatly, the size of carbides became thin, and no lamellar carbides appeared. In the samples with spheroidization annealing time of 90 minutes, the amount of carbides decreased, the size of carbides became large, and new lamellar carbides appeared. Therefore, it was concluded that lamellar carbides appeared in the later cooling stage.

It can be obtained from above results that the holding time of the sample 7# for the dissolution of carbides is long, whereas

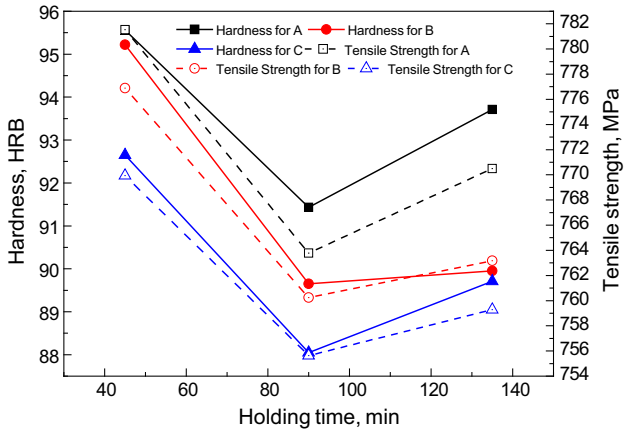

Fig. 7 Relationship between the hardness, tensile strength and t_1

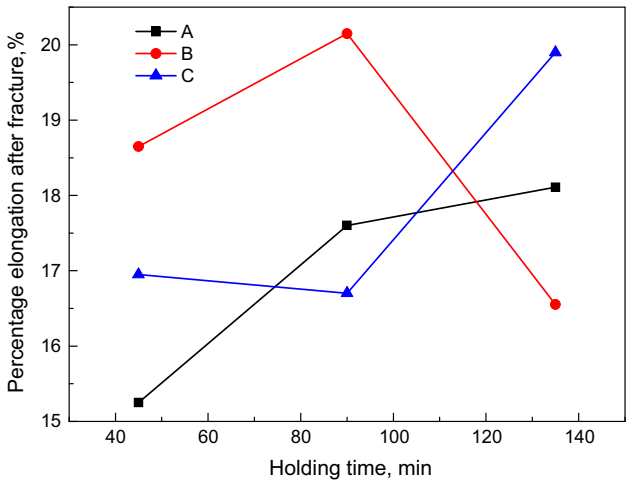

Fig. 8 Relationship between elongation after fracture and t_1

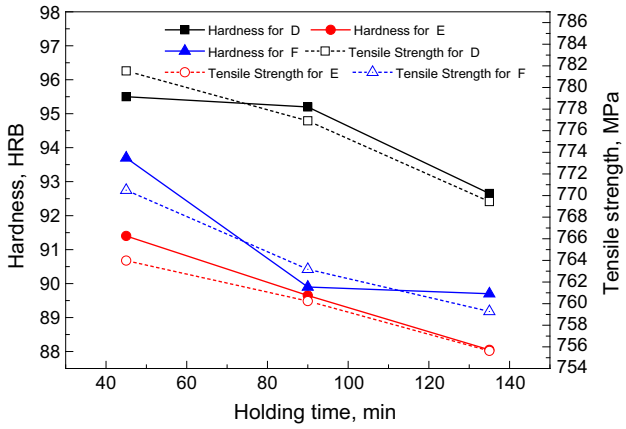

Fig. 9 Hardness and tensile strength of steel samples at various t_2

the holding time of spheroidizing is short. The redundant alloying elements, which dissolved into the matrix, cannot fully diffuse into the core of carbide. They precipitated as fine carbides and lamellar carbides at the large spacing in the end of the cooling process. These carbides would increase the hardness of matrix, and the tensile strength also increased (Ref 4). The holding time of spheroidizing t_2 for sample 8# was 90 min, which was twice compared with 7# sample. Therefore, there was no obvious increase in lamellar carbides in 8# sample. But compared with 5# sample, the matrix of sample 8# still contained many alloying elements. Part of these alloying elements was retained in the steel matrix during cooling, whereas others precipitated nearby or at the large spacing. These fine carbides could strengthen the steel matrix. The holding time of spheroidizing for sample 9# was 135 min. The spheroidization of carbides was sufficient under this condition. Therefore, there were no alloying elements that precipitated as lamellar carbides and fine carbides in the cooling process.

The above analysis showed that the formation of lamellar and fine carbides became easier with decreasing spheroidizing time. It was considered that the regular change was deduced on the condition of different cooling rates. Therefore, the samples with $t_1 = 135$ min and $t_2 = 45$ min were studied under the condition of different cooling rates.

SEM images of samples cooled at different cooling rates are shown in Fig. 11. Lamellar and spherical carbides were observed in each sample. With increasing cooling rate, the size of spherical carbides and lamellar carbides became smaller greatly, and the amount of lamellar carbide increased. The thickness and mean spacing of carbides in samples with largest cooling rate decreased by about 50% and the amount of carbide increased by 19.53% compared with that in the samples with smallest cooling rate. Some fine carbides in samples with the cooling rate of 250 °C/h appeared between spherical carbides. The minimum size of fine carbides was less than 20 nm. This result is consistent with the theoretical analysis.

4.2 Effect of Austenitizing Time on the Hardness

The heating process of 8Cr13MoV is similar with the high-temperature tempering of high-carbon martensitic steel. A large amount of carbides precipitate from martensite result in the decrease in hardness of material, but these carbides also play a hardening role to some extent in the matrix. When the samples were heated up to Ac_1 and hold, matrix transformed austenite has higher solubility on carbon. Some small carbides were also dissolved, and the remaining carbides would become the nucleation core of newly generated carbides after the heat preservation. When the t_1 was 45 min, the amount of small carbides was obviously higher than that in other samples, as shown in Fig. 10. These small carbides were partly precipitated in the heating process directly, and the others were derived from those segmented carbides. When t_1 was short, the amount of small carbides is greater after the lamelliform and long striped carbides were dissolved. The effect of hardening is more significant, so the hardness was higher than that of other samples. With increasing t_1, the small carbides were dissolved in the matrix, which resulted in the reduction in reinforcement and decrease in hardness. When t_1 was 90 min, the hardness of samples decreased to the minimum. When t_1 was 135 min, more carbides were dissolved into the matrix, which resulted in the decrease in nucleation core for carbides and the increase in alloying elements contents in the matrix. Under the same cooling condition, the decrease in spheroidizing degree of carbides could keep more alloying elements in the matrix, which played an important role in strengthening matrix. As a result, the hardness and tensile strength increased again.

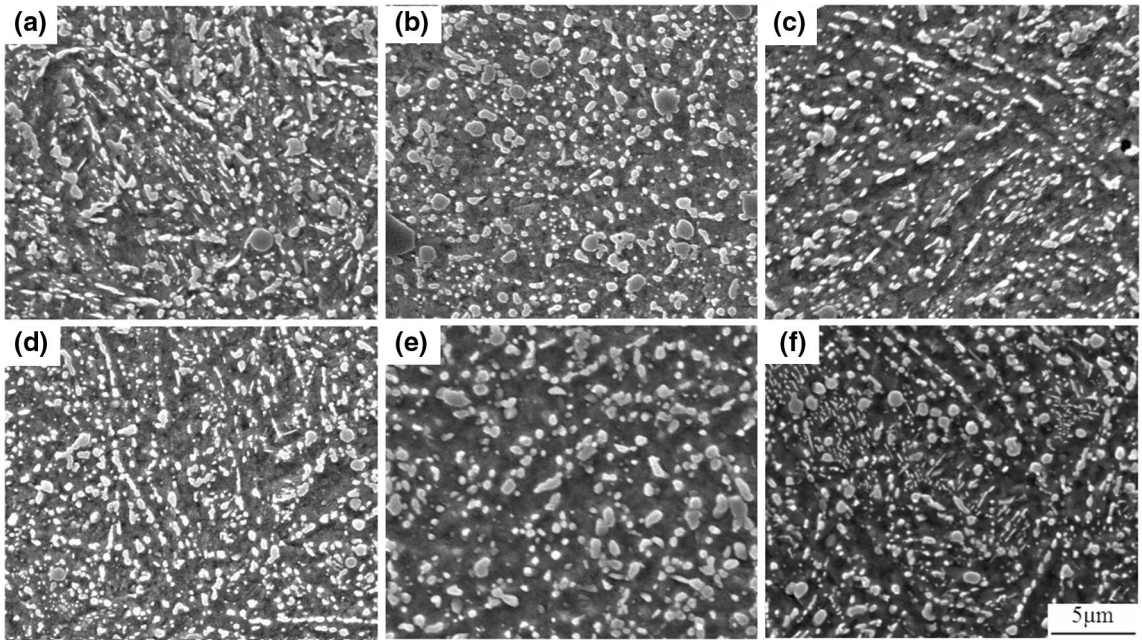

Fig. 10 SEM images of samples at different heating time in spheroidizing process: (a) t_1 = 45 min; (b) t_1 = 90 min; (c) t_1 = 135 min; (d) t_1 = 135 min, t_2 = 0 min; (e) t_1 = 135 min, t_2 = 90 min; (f) t_1 = 135 min, t_2 = 90 min, and cooling time = 120 min

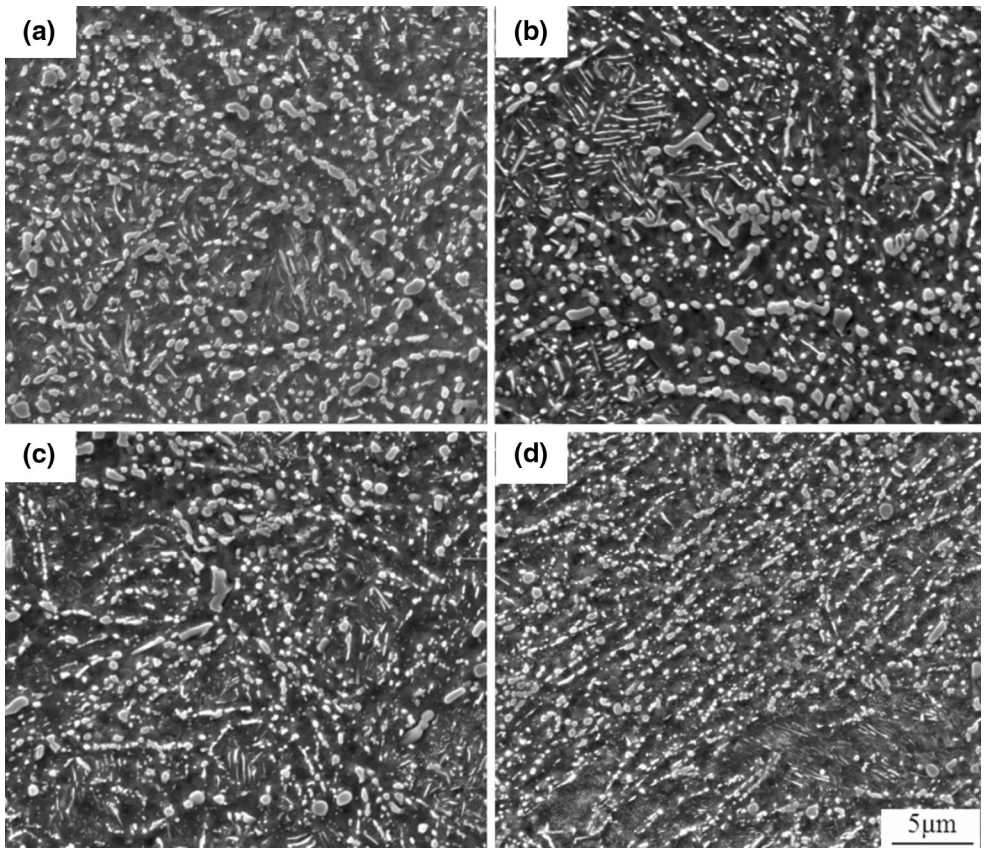

Fig. 11 SEM images of the samples cooled at different cooling rates: (a) 25 °C/h, (b) 50 °C/h, (c) 100 °C/h, (d) 250 °C/h

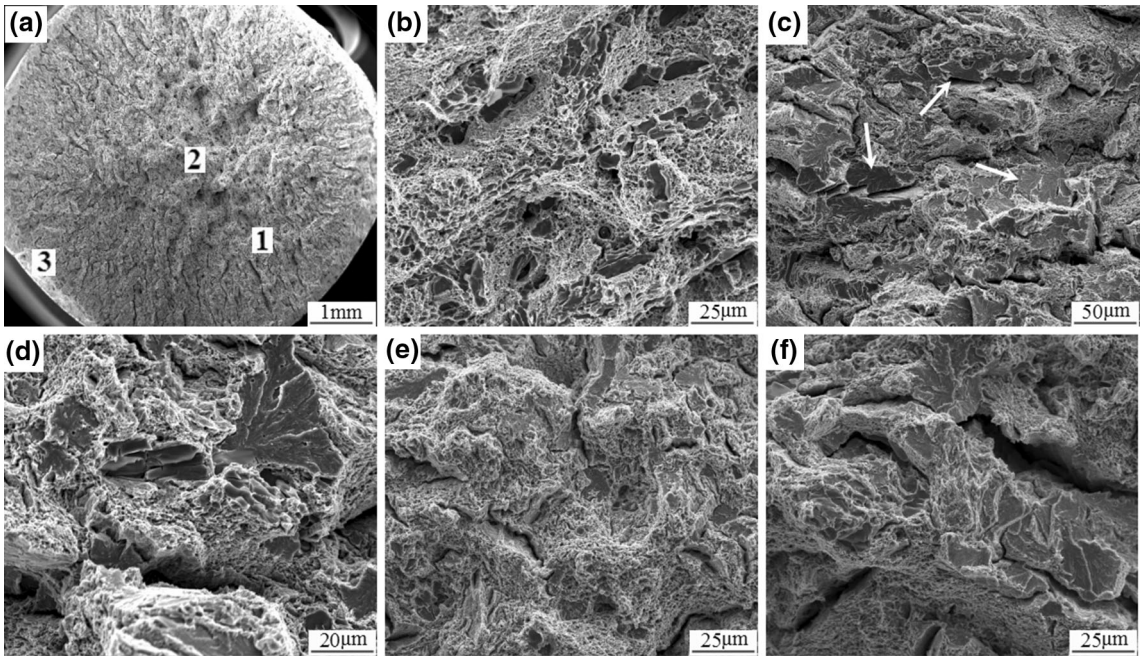

Fig. 12 SEM images of tensile fracture morphology: (a) overall morphology of a specimen, fiber area (b), radiation area (c), enlarged view of white arrow pointed location in image (c, d), crack spreading zone of specimen 5# (e), crack spreading zone of specimen 6# (f)

4.3 Influence of Austenitizing Time on the Growth Rate of Carbides at Spheroidizing Stage

In group D, E and F, there is a great difference in the spheroidization rate when t_2 was changed. It can be attributed to the difference in t_1. According to LSW theory (Ref 19), the radius of carbides and time during spheroidization process have the following relationship:

$$\frac{\mathrm{d}r}{\mathrm{d}t} = \frac{2D_M C_0^{\alpha}\sigma_S V_{\mathrm{m}}^{\alpha}}{r\left[C^{\beta} - C_r^{\alpha}\right]KT}\left[\frac{1}{\bar{r}} - \frac{1}{r}\right] \qquad \text{(Eq 1)}$$

where D_{M} represents the diffusion coefficient of alloying element in matrix, $\bar{r}$ represents the average radius of particles, C^{β} represents the carbides concentration, K is the gas constant. T is absolute temperature, V_{m}^{α} is partial molar volume of precipitates, σ_S is interfacial energy of carbides and matrix. It can be found from this formula that carbides whose radius is larger than average radius could grow up, while the carbides with the radius smaller than average radius would disappear. Hu et al. (Ref 20) obtained the instant growing rate formula of carbides in the spheroidization process, which took the diffusion of multiple component into consideration.

$$\frac{\mathrm{d}r}{\mathrm{d}t} = \frac{2V_{\mathrm{m}}^{\alpha}\sigma_S}{LKT}\frac{1}{r}\sum_{\mathrm{M}}\frac{D_{\mathrm{M}}}{k_{\mathrm{M}} - k_{\mathrm{Fe}}} \qquad \text{(Eq 2)}$$

where L is diffusion radius, k_{M} and k_{Fe} represent the distribution coefficient of alloying element and Fe in carbides and matrix, respectively, namely $k_{\mathrm{M}} = X_{\mathrm{M}}^{\beta}/X_{\mathrm{M}}^{\alpha}$ and $k_{\mathrm{Fe}} = X_{\mathrm{Fe}}^{\beta}/X_{\mathrm{Fe}}^{\alpha}$. According to this formula, the instant growing rate of carbides is inversely proportional to L. This means that the greater of the carbides spacing is, the slower of the instant growing rate is. The instant growing rate of carbides is also inversely proportional to $(k_{\mathrm{M}} - k_{\mathrm{Fe}})$. The instant growing rate decreases with increasing $(k_{\mathrm{M}} - k_{\mathrm{Fe}})$. In addition, it can be obtained that the instant growing rate increases with the increase in the concentration of the alloying element.

It can be obtained that holding time of austenitizing t_1 affects L and $(k_{\mathrm{M}} - k_{\mathrm{Fe}})$ directly. In the dissolution process of carbides, with increasing t_1, both carbides spacing and the concentration of alloying element increased. These two parameters had opposite effect on the growing rate. The experimental results showed that the spheroidization rate is in the order of $V_{\mathrm{F}} > V_{\mathrm{E}} > V_{\mathrm{D}}$ in the earlier stage of spheroidization process. It was deduced that the alloying element concentration had a larger effect on the spheroidization rate of carbides. With the increase in t_2, the concentrations of alloying elements in matrix decreased, and the spheroidization rate also decreased. The difference in the hardness between samples 5# and 6#, and that between samples 8# and 9# decreased, which was coincident with formula (2). The hardness change of D group increases, which may be attributed to short of t_1. There were many lamelliform carbides without sectional dissolution and some undissolved small carbides in the microstructure. In the early stage of t_2, the concentration of alloying element in the matrix is low. With the drive of interfacial free energy, the lamelliform carbides and some undissolved small carbides were still in the process of dissolution. At this stage, the spheroidization rate was small, and the change of steel hardness is not obvious. Di et al. (Ref 21) derived the instance growing rate formula of lamelliform carbides on the principle of dynamics.

$$\frac{\mathrm{d}r}{\mathrm{d}t} = \frac{2V_{\mathrm{m}}^{\alpha}\sigma_S C_0}{l_0 KT}\left(\frac{1}{r_1} - \frac{1}{r_2}\right) \qquad \text{(Eq 3)}$$

where l_0 is the length of lamelliform carbides, C_0 is the equilibrium concentration of alloying element at the position of carbides where the radius of curvature is zero. r_1 and r_2 are radius when the carbides coarsen to the curvature of ρ_1 and

ρ_2, respectively. According to the formula, the instant growing rate of carbides is inversely proportional to l_0. With the breaking of carbides, l_0 decreased, while the instant growing rate increased gradually. Therefore, the spheroidization rate of samples in group D increased gradually with the increase in t_2, which is different from those in other two groups.

4.4 The Irregular Change of Percentage Elongation After Fracture

The samples 5# and 6# in group E were selected to observe the tensile fracture. The hardness of sample 6# was the lowest, while the elongation after fracture was lower than that of sample 5#. The SEM images of tensile fracture in these two samples are shown in Fig. 12. The fracture was typical ductile fracture, which presented a cup-cone shaped feature. The macroscopic fracture of tensile sample is shown in Fig. 12(a), in which point 1 was crack spreading zone, point 2 was fibrous zone, and point 3 was shear lip alone. The microstructure of 8Cr13MoV after forge and anneal consists of ferrite and carbides. Ferrite has good ductility, while carbides have no ductility. Therefore, in the tensile process, the cracks were easily formed in the position where large primary carbides existed. The enlarged photograph of fibrous zone is shown in Fig. 12(b). There were many primary carbides and dimples distributed on the fracture. Because of hot working process, primary carbides were distributed along a certain direction. In the fibrous zone, cracks were produced at the places where these primary carbides existed, and then the cracks resulted in fracture. The enlarged photograph of radiation area is shown in Fig. 12(c), and this was different from that in fibrous zone. Except dimples and large primary carbides, there existed another quasi-cleavage fracture in this area. This fracture had the characteristic of river pattern, which is shown in Fig. 12(c). When it was enlarged partly, some different characteristics compared with quasi-cleavage fracture were found. Though it presented river pattern, the interior was not smooth. It presented arborization, which is shown in Fig. 12(d). Judging from the appearance, there were some secondary carbides precipitated along grain boundary, which presented arborization. This fracture was occurred on the carbides precipitated along grain boundary, which belong to intergranular fracture. The microstructure of crack spreading zone in sample 5# and 6# is shown in Fig. 12(e) and (f), respectively. The cracks in sample 5# were less than that in sample 6# obviously. It indicates that that the secondary carbides precipitated at grain boundaries in sample 5# were less than that in sample 6#.

It was concluded that the main factor that affected elongation after fracture remained the precipitation of carbides at grain boundaries. The formation of carbides was directly associated with element segregation (Ref 22-24). During the electroslag remelting process, the cooling intensity of position near mold was larger. Therefore, the element segregation is smaller at the position. Consequently, the amount of primary carbides was smaller, the segregation was more serious at the center of ingot, which resulted in more amount of primary carbides formation. During heat treatment process, the precipitation of secondary carbides is also related to this segregation of alloying elements. More secondary carbides will precipitate at the position where a large amount of primary carbides exist (Ref 25). For this reason, it was found that samples 5# and 9#, which were taken from the edge of ingot, had the maximum percentage elongation after fracture. The sample 6# was obtained from the center of remelted ingot.

5. Conclusions

1. The hardness of annealed 8Cr13MoV steel decreases first and then increases with increasing the austenitizing time. In the case where the holding time of austenitizing is too short, the formation of fine carbides during heating would strengthen the steel matrix. If the holding time is too long, more carbide-forming alloy elements will dissolve in matrix. These alloy elements also precipitate as lamellar carbides or fine carbides, which will increase the hardness of the steel.
2. The growth rate of carbides spheroidization increases with increasing the holding time of austenitizing. The effectiveness of carbides spheroidization was improved, and the hardness of the steel decreases with increasing the holding time of spheroidizing. Increasing the holding time of austenitizing or cooling rate at the final stage promoted the formation of lamellar carbides and fine carbides. On the contrary, increasing the holding time of spheroidizing or decreasing the cooling rate at the final stage could eliminate these carbides.
3. The optimum holding times of austenitizing and spheroidizing for obtaining the lowest hardness of steel are 90 and 135 min, respectively.
4. The holding times of both austenitizing and spheroidizing have a negligible influence on the elongation after fracture. The elongation after fracture increases with the decrease in the amount of secondary carbides precipitated at grain boundaries.

Acknowledgments

This work was financially supported by the National Natural Science Foundation of China (Grant Nos. 51444004 and 51574025). The financial support by the Project of High-tech Ships of Ministry of Industry and Information Technology of the People's Republic of China [Grant No. (2014)508] is also acknowledged.

References

1. D.H. Mesa, A. Toro, A. Sinatora, and A.P. Tschipschin, The Effect of Testing Temperature on Corrosion-Erosion Resistance of Martensitic Stainless Steels, *Wear*, 2003, **255**, p 139–145
2. D.V. John, H.P. Alfred, and F.C. Howard, Wear Tests of Steel Knife Blades, *Wear*, 1093, **2008**, p 265
3. Q.T. Zhu, J. Li, C.B. Shi, and W.T. Yu, Effect of Quenching Process on the Microstructure and Hardness of High-Carbon Martensitic Stainless Steel, *J. Mater. Eng. Perform.*, 2015, **24**(11), p 4313–4321
4. N.G. Zhao, Z.G. Yang, and Y.L. Feng, *Solid Phase Transformations in Alloys*, Central South University Press, Changsha, 2008, p 134
5. D. Yao, J. Li, J.H. Li, and Q.T. Zhu, Effect of Cold Rolling on Morphology of Carbides and Properties of 7Cr17MoV Stainless Steel, *Mater. Manuf. Process*, 2015, **30**, p 111–115
6. D.L. Li, D.S. Ma, Z.Z. Chen, H. Ji, B.S. Liu, A.J. Kuang, and Z.L. Zhan, Spheroidizing Annealing Process of 7CrMn2Mo Steel, *Heat Treat. Met.*, 2010, **35**, p 57–61
7. G.E. Totten, *Steel Heat Treatment Metallurgy and Technologies*, CRC Press, Boca Raton, 2007, p 201
8. J.D. Verhoeven and E.D. Gibson, The Divorced Eutectoid Transformation in Steel, *Metall. Mater. Trans. A*, 1998, **29**, p 1181–1189

9. J.D. Verhoeven, The Role of the Divorced Eutectoid Transformation in the Spheroidization of 52100 Steel, *Metall. Mater. Trans. A*, 2000, **31**, p 2431–2438
10. F.J. Hui, H. Dong, Q.Y. Weng, M.Q. Wang, S.L. Chen, and J. Shi, Effect of Heat Treatment Parameters on Mechanical Properties of High Strength Cr-Mo-V Steel, *Acta Metall. Sin.*, 2002, **10**, p 1009–1014
11. H.J. Li, B.Q. Wang, X.Y. Song, S.Z. Guo, and N.J. Gu, New Spheroidizing Technique of Ultra-High Carbon Steel with Aluminum Addition, *J. Iron. Steel Res. Int.*, 2006, **13**, p 9–13
12. W.T. Yu, J. Li, C.B. Shi, and Q.T. Zhu, Effect of Electroslag Remelting Parameters on Primary Carbides in Stainless Steel 8Cr13MoV, *Mater. Trans*, 2016, **57**(9), p 1547–1551
13. W.T. Yu, J. Li, C.B. Shi, and Q.T. Zhu, Effect of Titanium on the Microstructure and Mechanical Properties of High-Carbon Martensitic Stainless Steel 8Cr13MoV, *Metals*, 2016, **6**(8), p 193
14. Y.L. He, N.Q. Zhu, X.Y. Hu, and L. Li, Thermodynamic and Kinetic Calculation on Precipitation Behavior of Chromium Carbide, *Trans. Mater. Heat Treat.*, 2001, **32**(1), p 134–137
15. J.M. Xiao, *The Metallography of Stainless Steel*, Metallurgical Industry Press, Beijing, 2006, p 101
16. Z.L. Song, X.D. Du, Y.Q. Chen, J.Q. Wang, C. Ye, and L.Y. Li, Microstructure and Impact Toughness of 7Cr17Mo Martensitic Stainless Steel, *Trans. Mater. Heat Treat.*, 2011, **32**, p 95–99
17. X. Wu, Z.X. Zhao, and R.D. Xue, Carbide behavior in 5Cr15MoV steel during the isothermal and slow cooling process of spheroidization annealing, *Trans. Mater. Heat Treat.*, 2014, **10**, p 98–102
18. N.V. Luzginova, L. Zhao, and J. Sietsma, The Cementite Spheroidization Process in High-Carbon Steels with Different Chromium Contents, *Metall. Mater. Trans. A*, 2008, **39**, p 513–521
19. Y.Z. Wu and L. Li, *Materials Thermodynamics*, Science Press, Beijing, 2000, p 173
20. X.B. Hu, L. Li, and X.C. Wu, Coarsening Kinetics of Carbides in 4Cr5MoSiV1 Hot Work Tool Steel During Thermal Fatigue, *Trans. Mater. Heat Treat.*, 2005, **01**, p 57–62
21. H. Di, X. Zhang, and G. Wang, Spheroidizing Kinetics of Eutectic Carbide in the Twin Roll-Casting of M2 High-Speed Steel, *J. Mater. Process. Technol.*, 2005, **166**, p 359–363
22. X.F. Zhou, F. Fang, G. Li, and J.Q. Jiang, Morphology and Properties of M2C Eutectic Carbides in AISI, M2, *ISIJ Int.*, 2010, **50**, p 1151–1157
23. V.I. Chumanov and I.V. Chumanov, Control of the Carbide Structure of Tool Steel During Electroslag Remelting: Part I, *Russ. Metall.*, 2011, **6**, p 515–521
24. N. Meilinda, T. Panos, and J.P. Eric, A Study of Carbide Precipitation in a H21 Tool Steel, *ISIJ Int.*, 2014, **54**, p 1667–1676
25. Q.T. Zhu, J. Ling, C.B. Shi, and W.T. Yu, Effect of Electroslag Remelting on Carbides in 8Cr13MoV Martensitic Stainless Steel, *Int. J. Min. Metall. Mater.*, 2015, **22**, p 1149–1156